Hydrocarbon Rocket Engines for Earth-to-Orbit Vehicles

James A. Martin*
NASA Langley Research Center, Hampton, Virginia

The Space Shuttle has initiated a new era in Earth-to-orbit transportation and studies are now under way to assess the technology requirements for more advanced vehicles. Potential derivatives of the Space Shuttle and completely new vehicles might both benefit from advanced hydrocarbon engines, several versions of which were recently studied. In the present paper, selected single-stage vehicles have been compared using these engines. The results indicate that propane staged-combustion engines are attractive for this application. The potential effects of advanced engine materials are also shown.

Introduction

THE Space Shuttle has initiated a new era in Earth-to-orbit transportation, and the large number of payload reservations indicates that the system will be used to capacity. Many advantages of operating in space with the Shuttle have been hypothesized, such as satellite checkout and repair in orbit. Assembly of large space structures from the Shuttle is also being considered. Beyond the first few years of the Shuttle era, Earth-to-orbit traffic will grow to the point that vehicles beyond the Space Shuttle should be developed for a more efficient transportation system. Advanced orbit-transfer vehicles are being considered in several future systems studies. Even though the Space Shuttle era has just begun, the time to develop the technology for future vehicles is now. Derivatives of the Space Shuttle have been studied in the past,[1] and a current study[2] will provide additional insight into such derivatives. For the more distant future, completely new, fully reusable vehicles have been proposed as in Refs. 3-6.

One of the more promising concepts that have been considered for new vehicles is the single-stage, dual-fuel vehicle. Vertical launch and horizontal landing, which is the operational mode of the Space Shuttle, may provide the lowest risk. One of the most significant design concerns for such a concept is the aft center of gravity. This concern is somewhat alleviated by dual-fuel propulsion, and recent work on control-configured design indicates that vehicles can be controlled during return from orbit to the runway with center-of-gravity locations considerably aft of the current Shuttle limits.[7]

Previous studies have shown that advanced hydrocarbon liquid rocket engines would be beneficial to both Shuttle derivatives and advanced vehicles. Replacing the Shuttle solid rocket boosters with liquid-fueled boosters could reduce environmental concerns and operational costs. Although derivatives of the Space Shuttle Main Engine (SSME) could be used for such liquid-fueled boosters, advanced hydrocarbon engines would reduce operational costs more. Several advanced hydrocarbon engines have been studied in the past for use with hydrogen-fueled engines for new Earth-to-orbit vehicles, and the results have indicated a significant advantage over hydrogen engines alone.[1]

One of the findings that surfaced in previous studies is that the proposed single-stage vehicle was most attractive when a tripropellant engine was assumed. Tripropellant engines get most of their thrust from the hydrocarbon fuel, and hydrogen is used for cooling or turbine power. Tripropellant engines that have been considered include dual expander and hydrogen gas-generator engines. A Shuttle liquid-booster derivative, on the other hand, would be significantly less attractive if hydrogen were required. Also, new two-stage vehicles might be better if no hydrogen were required in the first stage. The requirement for including hydrogen in first stages would be an additional complexity.

In order to provide an improved data base for vehicle evaluations, several hydrocarbon engines were recently studied (see Appendix and Ref. 8). The purpose of the study reported in this article was to compare single-stage Earth-to-orbit vehicles which use these hydrocarbon engines.

Reference Vehicle

The reference vehicle selected for the comparisons is described in considerable detail in Ref. 4. It was selected because of the design depth and because it has the most likely characteristics for the first new Earth-to-orbit vehicle after the Space Shuttle. The accelerated-technology vehicle was selected rather than the normal-growth-technology vehicle from Ref. 4.

In order to establish the relationship between the analysis methods of the current study and those used in the study of Ref. 4, the reference vehicle was first analyzed with the engines selected in that study. Those engines were dual-expander[9] engines with methane and hydrogen fuel. As Fig. 1 shows, the methods of the current study agree reasonably well (within 4%) with the reference vehicle dry mass at the same hydrocarbon propellant fraction, 0.61. The hydrocarbon propellant fraction is the ratio of the sum of the hydrocarbon fuel mass and the mass of the oxygen burned with the hydrocarbon fuel to the total propellant mass. Figure 1 also shows that the dry mass can be reduced more than 15% if the hydrocarbon propellant fraction is optimized. Computer-aided design techniques used in the current study allow more optimization than could be accomplished in the study of Ref. 4. The hydrocarbon propellant fraction is varied by changing the time at which the hydrocarbon portion of the engine is turned off. The hydrogen portion of the engine operates in parallel with the hydrocarbon portion initially and alone after the hydrocarbon portion is turned off.

Analysis Methods

The analysis methods of the current study are similar to those of previous studies[1,3,5,7] except that additional computer programs have been added to facilitate the large number of engine parametrics considered. As shown in Fig. 2, engine data (specific impulse, mass, etc.) are stored in one computer file and case data (types of engines, hydrocarbon propellant fraction, etc.) are stored in another computer file. The user selects the case to be analyzed, and a trajectory input file is created and sent to the Program to Optimize Simulated Trajectories (POST).[10] The trajectory analysis program operates on a mainframe computer; all other computer programs operate on a minicomputer. The result of interest from the trajectory calculation is the ratio of gross mass to burnout mass. This ratio and the corresponding case selection are then used to provide the input to the vehicle sizing and mass estimation iteration. These procedures are essentially the

Presented as Paper 81-1371 at the AIAA/SAE/ASME 17th Joint Propulsion Conference, Colorado Springs, Colo., July 27-29, 1981; submitted Aug. 12, 1981; revision received Jan. 3, 1983. This paper is a work of the U.S. Government and therefore is in the public domain.

*Aerospace Engineer, Space Systems Division. Member AIAA.

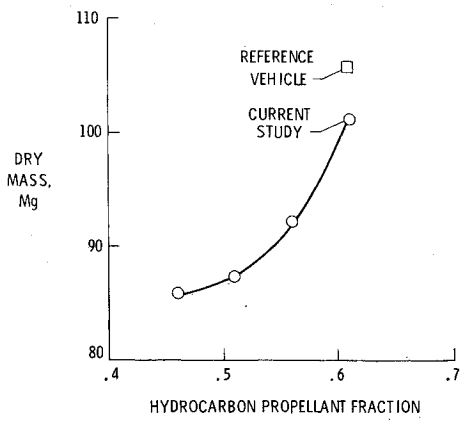

Fig. 1 Reference vehicle comparison.

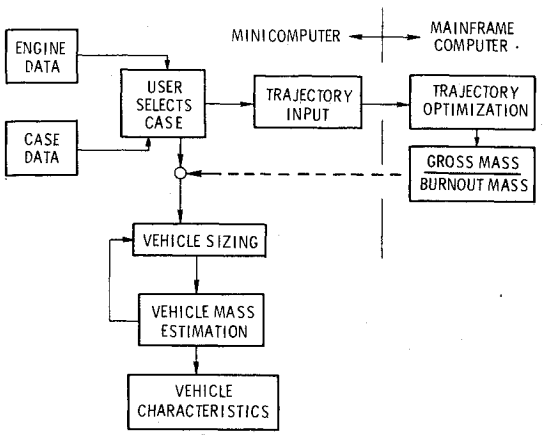

Fig. 2 Analysis methods.

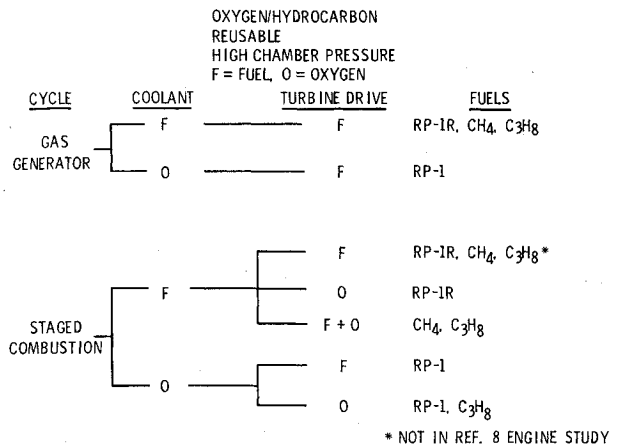

Fig. 3 Engines considered.

same as those of the Aerospace Vehicle Interactive Design (AVID) system of computer programs.[11] When a converged vehicle design is achieved, the vehicle characteristics are printed.

Except for the comparisons with the reference vehicle presented on Fig. 1, all of the vehicles analyzed were parallel-burn concepts. At liftoff, the hydrocarbon engines were operated simultaneously with modified Space Shuttle Main Engines (SSMEs). The modification was that the expansion ratio was changed to 40 for the initial phase of the flight and that a nozzle extension for an expansion ratio of 150 was added for the final portion of the flight. The nozzle extension was used after the hydrocarbon engines were turned off. For the initial portion of this paper, a hydrocarbon thrust fraction

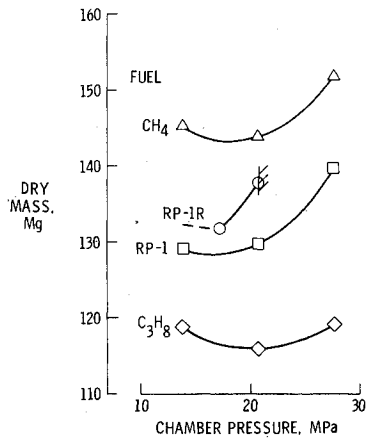

Fig. 4 Chamber pressure optimization for gas-generator engines.

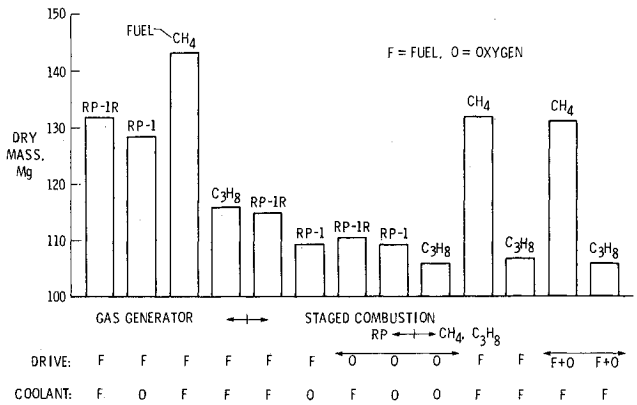

Fig. 5 Preliminary screening results.

of 0.8 and a hydrocarbon propellant fraction of 0.79 were assumed; these parameters are discussed further in the section on vehicle parametric optimization. These parameters can affect the results, but the trends shown at representative values should be valid. Optimizing these parameters for each case would be prohibitive in computer and manpower costs.

Preliminary Screening

The first phase of this study was a preliminary screening in order to reduce the number of engines for further study. The matrix of engines considered is shown in Fig. 3. Both gas-generator and staged-combustion cycles were considered. Fuel and oxygen were considered as coolants. Turbine-drive gases were rich in fuel, oxygen, or both fuel and oxygen. The fuels were methane (CH_4), subcooled propane (C_3H_8), RP-1, and a highly refined grade of RP-1 called RP-1R. In the engine study,[8] RP-1 was considered as a coolant and was found to be quite poor, so RP-1R was added for use on fuel-cooled engines because it is a better coolant. No vehicle analyses were performed using engines with RP-1 cooling. No gas-generator cycles were analyzed using oxygen-rich, turbine-drive gases; these were considered briefly in the engine study and dropped because the turbine mass flow is greater than the mass flow for fuel-rich turbine drive.

The first step in the preliminary screening was optimization of the chamber pressure for the gas-generator engines. The results of this optimization are shown in Fig. 4. Vehicle dry mass is used as the characteristic to be minimized because previous results[1] indicated that it is a good compromise of minimum development costs, minimum life-cycle costs, and minimum gross mass. The engine with RP-1R cooling is limited to a maximum chamber pressure of about 21 MPa, and only vehicle design points were calculated. At lower

chamber pressures, the results would follow the trend of the RP-1 engines.

Figure 5 shows the preliminary screening results. The gas-generator results on the left represent the minimums of the curves of Fig. 4. The staged-combustion engines were all evaluated with a chamber pressure near the maximum possible value from the engine study, which is later shown to be optimum. Arrows denote two groups of engines that do not have just fuel-rich drive gases. Three conclusions are obvious:

1) Methane results in the highest vehicle dry mass for single-stage vehicles. Because of its low density compared to the other hydrocarbons, the vehicle must be considerably larger. The methane engines also have a higher mass because of methane's low density.

2) The gas-generator cycles result in higher vehicle dry mass than the staged-combustion cycles, which is basically due to the low specific impulse inherent in gas-generator cycles. A tripropellant engine with a hydrogen-rich gas generator (not considered in the present study) overcomes this problem somewhat because of the high energy of hydrogen, but hydrocarbon gas-generator losses are significant. For example, an RP-1 engine with a delivered vacuum specific impulse of 331.6 s has a main chamber specific impulse of 349.4 s (Ref. 8).

3) Propane staged-combustion engines result in slightly lighter vehicles than those using RP-1 staged-combustion engines. Both RP-1 and propane staged-combustion engines were examined further in this study.

The results of Fig. 5 differ somewhat from the vehicle results in Ref. 8, particularly for methane fuel. A difference occurs because the vehicle used for comparisons in Ref. 8 was a large two-stage ballistic vehicle that was not affected as much by the volume requirements of methane fuel or the engine mass. The vehicle analysis of Ref. 8 also assumed a constant gross mass and calculated the payload, which tends to increase the importance of the hydrocarbon specific impulse. Even with these assumptions, engines using propane and methane fuels with the same engine cycle yielded equal payloads in Ref. 8.

Engine Parametric Optimizations

For the next phase of the study, the RP-1 and propane staged-combustion engines were evaluated at a variety of chamber pressures and expansion ratios. All of the engines in the previous preliminary screening had an expansion ratio that resulted in an exit pressure of 41 kPa (used in Ref. 8). There are slight differences between the preliminary data used for the initial screening and the detailed parametric data presented in Ref. 8, so the results in the remainder of this paper do not agree exactly with the results just shown in the preliminary screening. The following parametric results are considered to be more accurate.

Figures 6 and 7 show the trajectory mass ratios achieved as a function of the expansion ratios. Figures 8-10 show the resulting vehicle dry-mass values. The trajectory results in Fig. 7 are valid for both propane engines (Figs. 9 and 10). The results of these parametric optimizations are presented in Figs. 11 and 12, where the vehicle dry mass is shown as a function of engine chamber pressure for each engine type. At each chamber pressure, the expansion ratio is selected to minimize dry mass. The maximum chamber pressure limit from Ref. 8 is also shown for each engine type.

The results in Figs. 11 and 12 for all engine types indicate that the optimum chamber pressure is the maximum and that there would be further gains if the chamber pressure could be increased. Although the trajectory mass-ratio results, as in Figs. 7 and 8, usually indicate an advantage to increasing both chamber pressure and expansion ratio, the vehicle design analyses reflect the penalty due to engine mass. In this case, there is an optimum in the expansion ratio (Figs. 8-10) because of the tradeoff between mass ratio and engine mass. Even with the engine mass penalty resulting from increasing

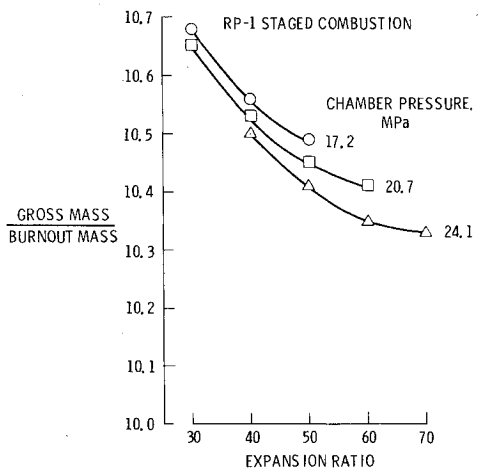

Fig. 6 Trajectory results with RP-1 staged-combustion engines.

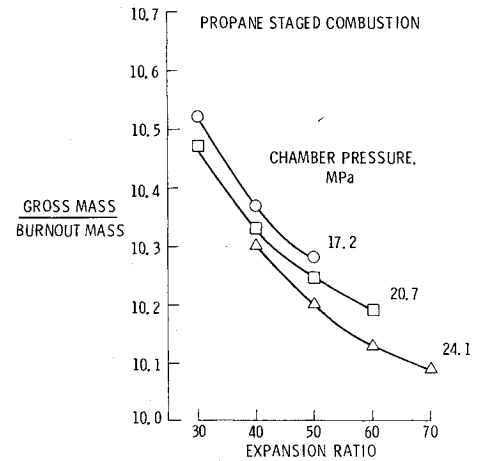

Fig. 7 Trajectory results with propane staged-combustion engines.

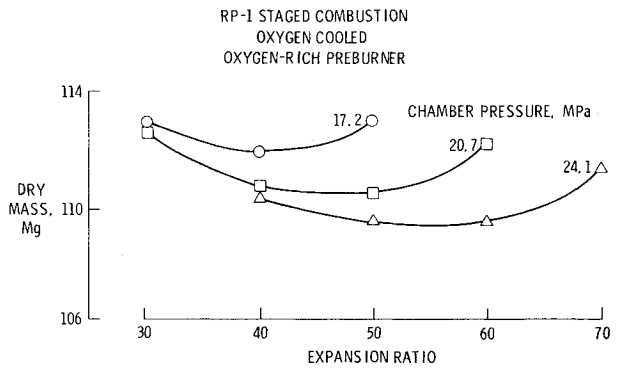

Fig. 8 Vehicle results with RP-1 engines.

chamber pressure, the results here indicate that the mass-ratio improvements have more effect than the engine mass increases in the range of interest for chamber pressure.

Only one RP-1 engine was analyzed at the preliminary design level in Ref. 8. In order to compare various cycles, the engine mass increment from the preliminary screening was used. One vehicle was evaluated using the modified engine mass, and the curve of Fig. 11 was offset accordingly. Comparing the two RP-1 engine types in Fig. 11 indicates that the oxygen-cooled engine has a slightly lower vehicle dry mass than the fuel-cooled engine, even though the fuel-cooled engine has a slightly higher maximum chamber pressure. This is because the fuel-cooled engine has a higher engine mass. The difference in engine mass between these two engine types is estimated to be 45 kg at the same chamber pressure and

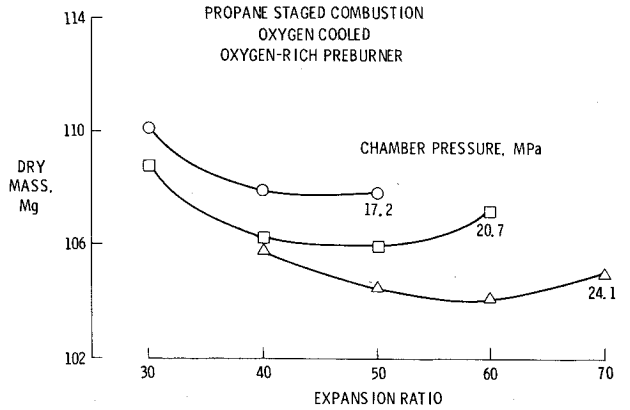

Fig. 9 Vehicle results with propane engines with oxygen cooling and oxygen-rich preburners.

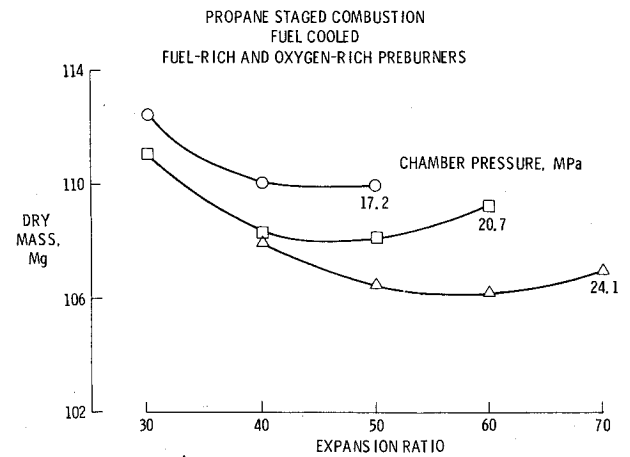

Fig. 10 Vehicle design results with propane engines with fuel cooling and fuel-rich and oxygen-rich preburners.

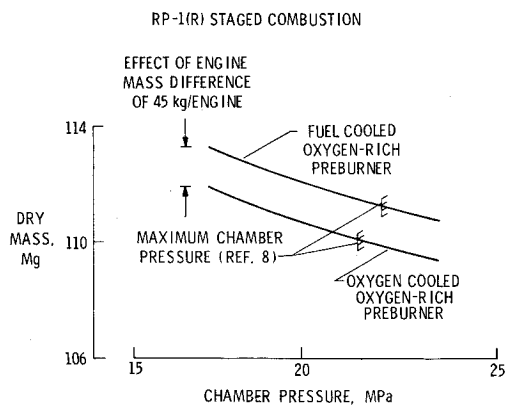

Fig. 11 Comparison of RP-1 staged-combustion engines.

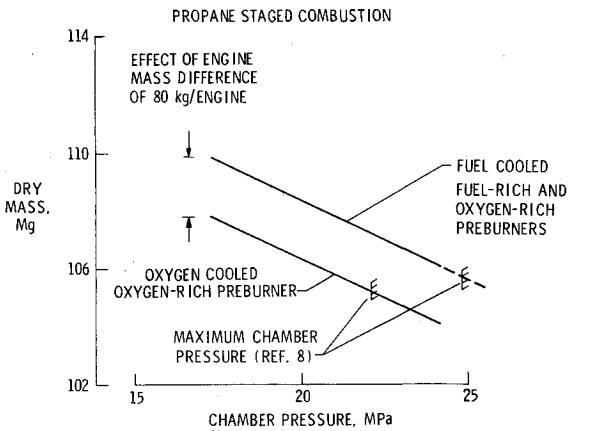

Fig. 12 Comparison of propane staged-combustion engines.

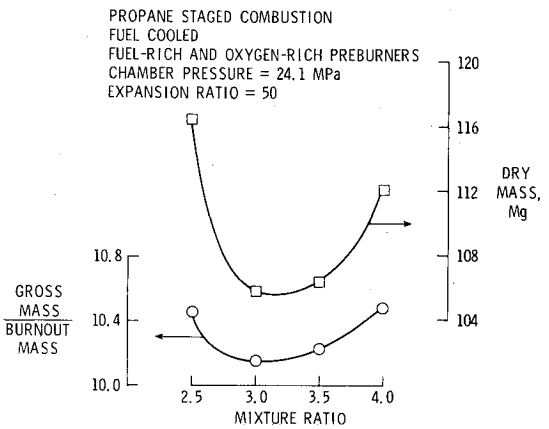

Fig. 13 Mixture ratio optimization.

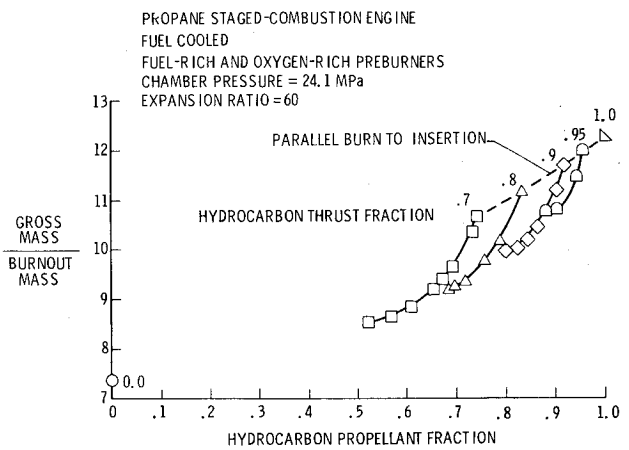

Fig. 14 Trajectory results for vehicle optimizations.

expansion ratio. Since the fuel-cooled engine was not studied beyond the preliminary screening level in the engine study, this difference is subject to some additional uncertainty. Two additional RP-1 staged-combustion engine types were considered. One has fuel cooling and a fuel-rich preburner. It has both a lower chamber pressure limit and a higher engine mass than the two engine types shown, so the vehicle dry mass is considerably higher. With an estimated engine mass 120 kg more than the oxygen-cooled, oxygen-rich preburner engine and a chamber pressure limit of 17.2 MPa, the vehicle dry mass is about 115.5 Mg. The other engine type has a fuel-rich preburner and oxygen cooling. The engine mass is estimated to be the same as that of the oxygen-cooled, oxygen-rich preburner engine, but the chamber pressure limit is lower (20.0 MPa). The vehicle dry mass is therefore higher (110.5 Mg). In summary, the comparison of vehicles using the four different RP-1 engines indicates that the three which use oxygen (for cooling, for an oxygen-rich preburner, or for both) result in vehicle dry-mass values that are within 1%, so selection of these engines should be based on other technology issues. The engine type that has fuel cooling and a fuel-rich preburner results in a 5% vehicle dry-mass penalty, so other types should be given preference.

Comparing Figs. 11 and 12 shows that the vehicle with a propane engine results in a lower dry mass than one with the RP-1 engines. The difference is about 4%. Because of this

Table 1 Engine characteristics

Fuel	RP-1	Propane	Propane
Cycle	Staged combustion Oxygen	Staged combustion Oxygen	Staged combustion Oxygen
Preburner	Oxygen-rich	Oxygen-rich	Fuel-rich and oxygen-rich
Expansion ratio	50	50	60
Chamber pressure, MPa	20.7	20.7	24.1
Vacuum specific impulse, s	351.6	358.3	361.7
Vacuum thrust, kN	3066.7	3056.3	3067.7
Exit area, m^2	3.925	3.822	3.915
Mass, kg	2136	2162	2332
Mixture ratio	2.8	3.1	3.1
Fuel density, kg/m^3	808.9	728.8	728.8
Oxygen density, kg/m^3	1140.5	1140.5	1140.5

difference and because propane is less expensive and has fewer potential problems than RP-1, the final portion of this study was limited to engines with propane fuel.

Figure 12 shows a comparison between two propane staged-combustion engine types. The first is oxygen-cooled and has an oxygen-rich preburner. The second is fuel-cooled and has two preburners. An oxygen-rich preburner provides power for the oxygen pump, and a fuel-rich preburner provides power for the fuel pump. Both of these engine types were studied in depth in the engine study.[8] The second engine type has a higher engine mass by 80 kg/engine, but the maximum chamber pressure is also considerably higher (24.82 vs 22.06 MPa). The resulting vehicle dry mass is very nearly the same for the two engines.

The second engine type was selected for the final part of this study for three reasons. First, it has a higher specific impulse and will therefore be preferred for applications where engine mass is not as important as the current single-stage application. Second, it has fuel cooling. The RP-1 analyses indicated that oxygen cooling yields a lower vehicle dry mass, so switching from fuel cooling to oxygen cooling may result in an improvement. On the other hand, oxygen cooling may be a more difficult technology development, so the fuel-cooled engine may be preferred. The third reason is that the two preburners eliminate the need for an interpropellant seal between a hot preburner gas, rich in one component, and a high-pressure liquid of the other component. In the SSME program, problems with the interpropellant seal resulted in the addition of a helium purge subsystem. The mass estimates of this study are based on the assumption that the need for a helium purge can be eliminated for future engines, but the possibility exists that a purge would still be required. The addition of a purge subsystem would significantly diminish the attractiveness of any engine requiring it by reducing the effective specific impulse, by the addition of the subsystem dry mass, and by the helium volume requirement. One technology that must be developed for the selected engine is an injector for two hot-gas streams; previous injectors have been for either two liquids or one gas and one liquid.

Figure 13 shows the results of a parametric study of mixture ratio, which is defined as the mass flow of the oxygen divided by the mass flow of the fuel. The trajectory mass-ratio results are a direct reflection of the vacuum specific impulse changes as a function of mixture ratio from Ref. 8. The vehicle dry-mass results reflect the specific impulse changes and the changes in tank volumes. A higher mixture ratio results in more oxygen mass, and, since oxygen is denser than propane, the optimum shifts slightly to the right. The baseline mixture ratio for propane engines was 3.1 for this study, which is nearly optimum. A more detailed optimization of mixture ratio is needed in the 3.0-3.5 range, with more engine effects included. The only effect included in this study was vacuum specific impulse. Changing mixture ratio could also affect the maximum chamber pressure, the engine mass, and the exit area.

Since Fig. 13 is plotted such that the dry-mass scale is exactly 10 times the mass-ratio scale, the sensitivity of dry mass to mass ratio can be seen by considering the points at mixture ratios of 3.5 and 4.0. If the trajectory is off optimum such that the mass ratio is high by 2%, the dry-mass results will be over 6% high.

As a result of these engine optimizations, three engines were selected as the most promising ones. The characteristics of these three engines, as used in the present study, are shown in Table 1.

Vehicle Parametric Optimization

As a result of the previous analyses, a propane engine was selected with fuel cooling, fuel-rich and oxidizer-rich preburners, and an expansion ratio of 60. The chamber pressure selected was 24.1 MPa because the engine characteristics were available[8] for this case rather than the maximum possible of 24.8 MPa.

All of the previous results of Figs. 4-13 were calculated with the assumptions that the hydrocarbon thrust fraction was 0.8, which means that 80% of the vacuum thrust came from the hydrocarbon engines, and that the hydrocarbon propellant fraction was 0.79. These values were based on the results of previous studies,[12] and these vehicle parameters were optimized only with the selected engine. The impact of the thrust fraction and propellant fraction is shown in Figs. 14 and 15.

The trajectory mass-ratio results shown in Fig. 14 indicate that there is a mass-ratio penalty associated with increasing either the hydrocarbon thrust fraction or the hydrocarbon propellant fraction. This is expected, since the specific impulse of the hydrocarbon engine is considerably less than that of the hydrogen engine. The upper points on each curve represent the limiting case in which both engine types are used in parallel for the entire ascent. A point is included which represents the all-hydrogen engine case.

Figure 15 shows the vehicle dry-mass results. The optimum is for a thrust fraction of 0.8 to 0.9, which indicates that the mass-ratio penalty for increasing hydrocarbon thrust fraction is more than offset by the reduction in engine mass and propellant volume. With a high hydrocarbon propellant and thrust fraction, there would probably be some benefit to adding a two-position nozzle to some of the hydrocarbon engines, but this was not examined in this study. The trajectory optimization was somewhat difficult for hydrocarbon thrust fractions of 0.9 and 0.95 and hydrocarbon propellant fractions near the optimums because the burn times became very long. Typical burn times for other cases were about 400 s, but these cases approached 600 s. This

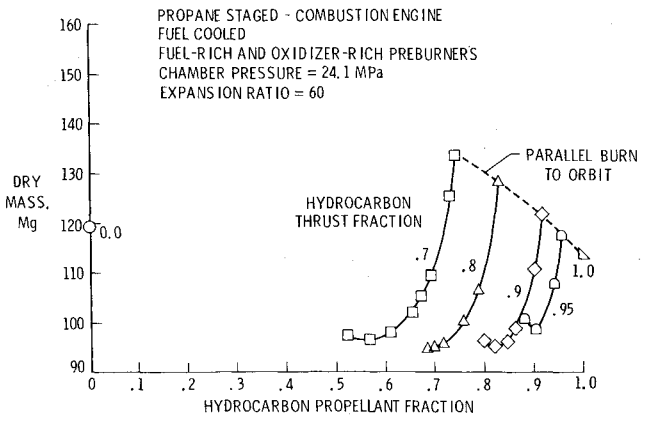

Fig. 15 Vehicle results for vehicle optimizations.

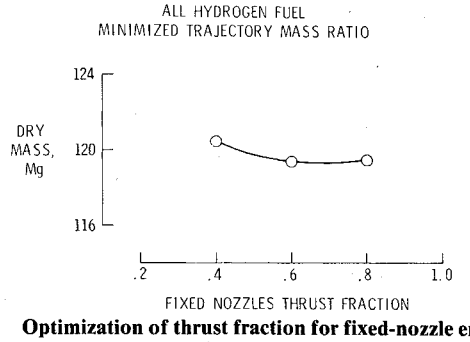

Fig. 16 Optimization of thrust fraction for fixed-nozzle engines.

happens because the hydrogen thrust is so low during the final phase of the trajectory. Additional trajectory analyses might reveal a way to improve these cases. In this study, all engines were throttled equally to avoid exceeding an acceleration of 3 times the Earth's gravity during the parallel-burn phase of the trajectory. Throttling the hydrogen engines first would improve the results.

Figures 14 and 15 both include an all-hydrogen point for reference. This point corresponds to a vehicle with some two-position nozzles and some fixed nozzles. The thrust fraction for the fixed-nozzle engines and the propellant fraction (propellant consumed before the fixed-nozzle engines were shut off and before the two-position nozzles were extended) were both optimized. Figure 16 shows the optimization of the thrust fraction with a minimum at 0.685. The propellant fraction was optimized within the trajectory optimization program.

Figure 15 also shows the importance of the correct selection of propellant fraction and thrust fraction. For example, a hydrocarbon thrust fraction of 0.8 and a hydrocarbon propellant fraction of 0.79 appeared to be reasonable values before the calculations were made, but these values resulted in a vehicle dry mass over 12% higher than the optimum. It is also important to achieve an optimum trajectory. All the points on Fig. 15 are for optimized trajectories.

As a result of the vehicle optimizations, one vehicle was selected as optimum. Some of the engine characteristics of this optimum vehicle are given on Fig. 15. The dry mass of this vehicle is 94.5 Mg, and the gross mass is 1195.4 Mg. The optimum hydrocarbon thrust fraction is 0.8, and the optimum hydrocarbon propellant fraction is 0.685.

Technology Assessments

The first technology to be assessed was engine materials. In the engine study,[8] a significant effort was made to assess the effect of advanced materials on engine mass. The original engine mass estimates were based on materials that have been

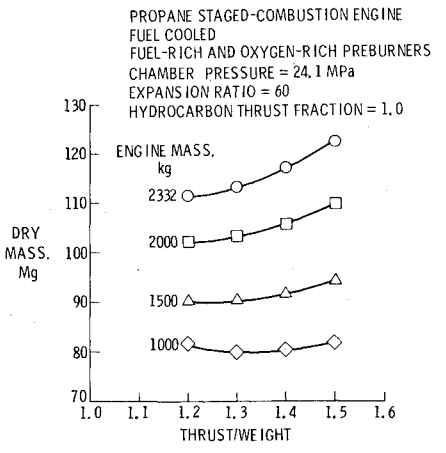

Fig. 17 Effect of engine mass on vehicle thrust-to-weight optimization.

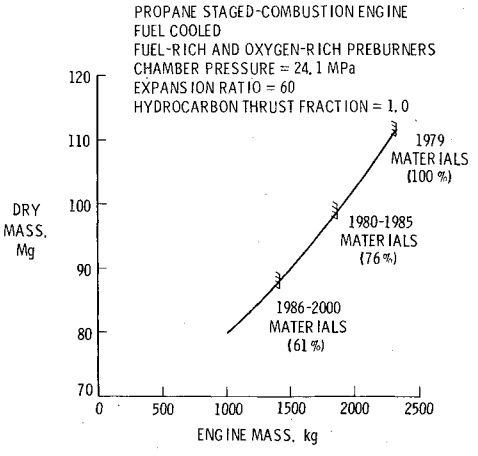

Fig. 18 Effect of advanced engine materials on vehicle dry mass.

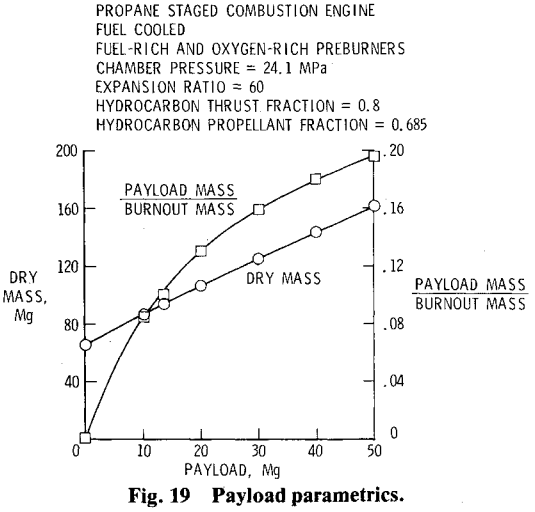

Fig. 19 Payload parametrics.

used in the past, such as those used in the SSME. In the future, new materials, particularly composites, could be used to reduce the engine mass below the original 1979 materials estimates.

In order to assess the impact of engine mass, the vehicle dry mass was calculated for a series of engine-mass values at several vehicle-liftoff thrust-to-weight values. The all-hydrocarbon vehicle was used, since improvements in the hydrocarbon engine would drive the optimization toward this vehicle. The results are shown in Fig. 17. The minimums of

each of these curves provided one point for Fig. 18, in which the vehicle dry mass is shown as a function of engine mass. Also shown on Fig. 18 are the engine mass estimates corresponding to advanced materials for two advanced time periods. The calculations on which these engine mass estimates are based are shown in detail in Ref. 8. The engine mass used for the other parts of this study is represented by the point labeled 1979 materials. An engine built in the near future could have a mass of about 76% of the mass of the engine built with 1979 materials (24% reduction). The corresponding vehicle dry mass is reduced about 11%. An engine built in the more distant future could have a mass of about 61% of the engine built with 1979 materials (39% reduction). The corresponding vehicle dry mass is reduced 21%. These are very significant savings, and engine-mass reductions should be pursued in technology developments, but additional research will be required to verify the feasibility of the individual mass-reduction items.

The technology areas assessed (other than engine mass) all result in increases in the engine chamber pressure limit for staged-combustion engines. Additional vehicle design calculations were not required for these assessments, since extrapolations of the curves of Figs. 11 and 12 provided the desired incremental values. The pump-discharge pressures were limited to 55 MPa for the engine study,[8] which is only slightly greater than the maximum existing in the SSME. Future engines, particularly engines without an interpropellant seal, will probably have somewhat higher maximum pressures. Assuming an optimistic increase to 70 MPa results in a chamber pressure increase from 24.8 to 28 MPa (Ref. 8) for the propane engine selected previously. From Fig. 12, this corresponds to a vehicle dry-mass reduction from 105.7-104.0 Mg, or 1.6%.

The next technology to be assessed was turbine inlet temperature. The engine study[8] did not assess this technology for the selected propane engine, so the effect was estimated for an RP-1 engine. Increasing the turbine inlet temperature from 922 to 1444 K for an oxygen-rich preburner increased the chamber pressure limit from 21.7 to 25 MPa. From Fig. 11, this corresponds to a vehicle dry-mass reduction from 111.2 to 110.6 Mg, or 0.5%.

The next assessment was to evaluate the impact of a carbon deposit on the combustion chamber wall. Hydrocarbon engines have been observed to have a carbon deposit at low chamber pressures, and there is some possibility that a carbon deposit could exist at higher chamber pressures with some engine designs. The benefit was shown in Ref. 8 to be about half of the benefit of the turbine inlet temperature increase evaluated previously, so the vehicle dry-mass reduction is expected to be less than 0.3%.

Applying these three changes to gas-generator engines has a greater impact than the results shown here for staged-combustion engines. The effect is to decrease the gas-generator losses and bring the specific impulse of gas-generator engines closer to that of staged-combustion engines, but there will always be some gas-generator loss. Overall, these technologies should be considered of lower priority than technology development for engine-mass reduction and development of a data base needed for propane staged-combustion engines.

Table A1 Engine characteristics

Engine mass, lb; RP-1 staged combustion; Oxygen cooled, oxygen-rich preburner; Sea level thrust = 600,000 lb									
Chamber pressure, lb/in.^{2}	Expansion ratio								
	30	35.6	40	41.3	42.5	46.7	50	60	70
2500	4436	4492[a]	4536	–	–	–	4635	4735	4834
3000	4539	–	4624	4635[a]	–	–	4709	4794	4879
3100	–	–	–	–	4633[a]	–	–	–	–
3500	4682	–	4757	–	–	4807[a]	4832	4906	4981

Engine mass, lb; Propane staged combustion; Fuel cooled, fuel-rich and oxygen-rich preburner; Sea level thrust = 600,000 lb								
Chamber pressure, lb/in.^{2}	Expansion ratio							
	30	36	40	41.7	47.2	50	60	70
2500	4651	4712[a]	4753	–	–	4855	4957	5060
3000	4768	–	4855	4870[a]	–	4942	5030	5117
3500	4913	–	4989	–	5044[a]	5065	5142	5218

[a] Nozzle exit pressure = 6 lb/in.^{2}.

Table A2 Engine specific impulse, s; staged combustion

Chamber pressure, lb/in.^{2}	Expansion ratio	RP-1 Oxygen/fuel = 2.8		Propane Oxygen/fuel = 3.1	
		Vacuum	Sea level	Vacuum	Sea level
2500	30	342.6	311.8	348.3	314.7
	40	347.6	305.0	354.0	309.7
	50	351.2	296.8	358.0	303.2
3000	30	343.0	315.7	348.8	321.8
	40	348.0	311.8	354.4	318.0
	50	351.6	306.0	358.3	312.9
	60	354.4	299.4	361.3	306.6
3500	40	348.4	317.0	354.8	323.8
	50	352.0	312.4	358.6	319.9
	60	354.8	307.2	361.7	314.9
	70	357.0	301.4	364.1	309.0

Payload Parametrics

Figure 19 shows the effect of varying the payload mass on the vehicle dry mass and on the ratio of payload mass to burnout mass on the selected vehicle. The payload volume was varied such that the payload density remained constant at 98.2 kg/m^3. The vehicle dry mass is almost linear with payload mass, but the vehicle dry mass is not zero at a payload mass of zero. Even when the payload mass and volume are zero, there are fixed-mass and fixed-volume items such as the crew compartment that must be included in the vehicle design. The ratio of payload mass to burnout mass can be thought of as the efficiency of carrying payload mass to orbit. At payload values near zero, the vehicle is very inefficient because the vehicle is carrying little payload compared to the fixed items. As the payload increases, the efficiency increases rapidly at first and continues to increase to payloads of 50 Mg.

Selecting the optimum payload mass for a vehicle can be a complex issue. The results of Fig. 19 show that a very small payload mass (0-10 Mg) may not be a good selection for delivering payload mass efficiently. On the other hand, larger vehicles would have larger development costs, and development costs are a significant part of discounted life-cycle costs for new Earth-to-orbit vehicles.[3] Another factor that should be considered is that the center of gravity of single-stage vertical-takeoff vehicles shifts aft (which aggravates entry control problems) as payload mass (and therefore gross mass) increases.[13] Also, producing a larger number of smaller vehicles can reduce costs because of the effect of learning on production costs.[14] Finally, the possibility of two new vehicles should be considered, one with a relatively small payload and one with a larger payload.[1]

Conclusions

The results of this investigation with pure hydrocarbon engines lead to the following conclusions for the single-stage Earth-to-orbit vehicle analyzed:

1) Of the fuels considered, propane is somewhat better than RP-1 and considerably better than methane in reducing vehicle dry mass.

2) Staged-combustion engines are better than gas-generator engines in reducing vehicle dry mass. Note that the use of tripropellant engines which include the use of hydrogen in the hydrocarbon engine could change this conclusion.

3) For RP-1 staged-combustion engines, using oxygen for cooling, for an oxygen-rich preburner, or for both is somewhat better than using fuel cooling and a fuel-rich preburner in reducing vehicle dry mass.

4) Engine mass reductions possible with advanced materials have a significant vehicle impact and should be pursued.

Appendix

Some of the engine characteristics needed for the analyses in this paper were not available in Ref. 8 and were provided by C.J. O'Brien of Aerojet Liquid Rocket Company. These characteristics are presented in Tables A1 and A2 for their reference value. All values are presented in the units provided.

References

[1] Martin, J.A., "Economic and Programmatic Considerations for Advanced Transportation Propulsion Technology," *Journal of Spacecraft and Rockets,* Vol. 17, Sept.-Oct. 1980, pp. 385-389.

[2] Williams, F., "Shuttle Derived Vehicles Technology Requirements Study," Contract NAS8-34183, Martin Marietta Corp., Rept. MMC-SDV-DR-3-6, Michoud Operations, 1981.

[3] Martin, J.A., "Cost Comparisons of Dual-Fuel Propulsion in Advanced Shuttles," *Journal of Spacecraft and Rockets,* Vol. 16, July-Aug. 1979, pp. 232-237.

[4] Caluori, V.A., Conrad, R.J., and Jenkins, J.C., "Technology Requirements for Future Earth-to-Geosynchronous Orbit Transportation Systems," NASA, CR 3265, April 1980.

[5] Eldred, C.H., Looking Toward Single-Stage Launch Systems," IAF Paper 80 F 242, Sept. 1980.

[6] Salkeld, R., Beichel, R., and Skulsky, R., "A Reusable Space Vehicle for Direct Descent from High Orbits," *Astronautics & Aeronautics,* Vol. 19, April 1981, pp. 46-47, 63.

[7] Freeman, D.C. and Wilhite, A.W., "Effects of Relaxed Static Longitudinal Stability on Single-Stage-to-Orbit Vehicle Design," NASA TP-1594, Dec.1979.

[8] O'Brien, C.J. and Ewen, R.L., "Advanced Oxygen-Hydrocarbon Rocket Engine Study," Aerojet Liquid Rocket Co., Rept. 33452F, Dec. 1980; also, see Appendix.

[9] Beichel, R., "The Dual-Expander Rocket Engine—Key to Economical Space Transportation," *Astronautics & Aeronautics,* Vol. 15, Nov. 1977, pp. 44-51.

[10] Brauer, G.L., Cornick, D.E., and Stevenson, R., "Capabilities and Applications of the Program to Optimize Simulated Trajectories (POST)," NASA, CR-2770, Feb. 1977.

[11] Wilhite, A.W. and Rehder, J.J., "AVID: A Design System for Technology Studies of an Advanced Transportation Concept," AIAA Paper 79-0872, May 1979.

[12] Martin, J.A. and Wilhite, A.W., "Dual-Fuel Propulsion: Why It Works, Possible Engines, and Results of Vehicle Studies," AIAA Paper 79-0878, May 1979.

[13] Freeman, D.C. Jr. and Powell, R.W., "Impact of Far-Aft Center of Gravity for a Single-Stage-to-Orbit Vehicle," *Journal of Spacecraft and Rockets,* Vol. 17, No. 4, July-Aug. 1980, pp. 311-315.

[14] Miller, R.H., "The Effect of Demand on Optimum Launch Vehicle Size," *Journal of Spacecraft and Rockets,* Vol. 16, July-Aug. 1979, pp. 287-288.